Interference Avoidance in Cognitive Radio Networks Using Cooperative Localization

Muhammad Farooq-i-Azam, *Member, IEEE,* Qiang Ni, *Senior Member, IEEE,* Mianxiong Dong, *Member, IEEE,* Haris Pervaiz, *Member, IEEE,* Charilaos Zarakovitis, *Member, IEEE,* and Fawaz Alsolami, *Member, IEEE*

***Abstract*—In the recent years, there has been a tremendous increase in the use of wireless medium and radio frequency spectrum due to the development of new types of wireless networks, applications and enabling technologies. Consequently, the radio frequency spectrum is getting over crowded due to this increasing demand. Traditionally, frequency bands are allocated to licensed users for their specific use. Cognitive radio allows secondary users to communicate using these frequency bands. However, this may result in interference to the primary users. Information of the relative positions of the primary and secondary users and the distance between them can be exploited to avoid this interference. In our work, we use cooperative localization strategy to determine the distance between the secondary and primary users. This distance information is then utilized to adjust the transmission power of the secondary nodes so that the interference threshold of the primary users is not exceeded. The proposed methodology is evaluated using simulation experiments. Different aspects of the proposed algorithm including location and distance estimation, channel availability and channel capacity against transmission power and path loss are evaluated. The results show that the proposed scheme is able to achieve considerable gains as a consequence of interference avoidance.**

***Index Terms*—interference, cognitive radio, localization, positioning, interference avoidance, frequency resources**

I. Introduction

MANY different types of wireless communication networks have been developed and deployed in the recent history. Examples of these networks include cellular [1], [2], sensor [3], [4], Internet of things (IoT) [5], [6] and wireless local area networks (WLAN) [7], [8]. An increased use of these wireless networks has resulted in a very high utilization of the wireless frequency resources. Traditionally, most of these frequency resources in a given geographic region are allocated to licensed users for their use as and when required. However, most of this licensed spectrum may remain underutilized due to inactivity of the primary user (PU). This leads to an inefficient use of the important frequency resources. Meanwhile, numerous applications which utilize wireless medium are being constantly developed. Consequently, these newer applications and networks [9] may fall short of required frequency resources.

Many options are being explored to address the problem of frequency spectrum scarcity. Some of these options include utilization of visible light communication (VLC) [10], tremendously high frequencies, such as, terahertz [11], device to device (D2D) communication [12], [13], and cognitive radio (CR) [14], [15]. Particularly, spectrum scarcity can be overcome by using the unique solution provided by CR. A CR is equipped with cognition and intelligence which enable it to sense the environment and thereby dynamically and adaptively modify its operating characteristics and parameters, such as, transmission power, modulation and frequency so as to dynamically and opportunistically access the frequency resources. The objective of a CR is to allow secondary users (SUs) to utilize the frequency bands which are otherwise allocated to licensed PUs so as to improve efficiency of spectrum usage. To dynamically and opportunistically access the frequency resources, either one or a combination of three communication modes, namely, overlay, underlay and interweave, can be used. However, this SU communication may cause interference to the PU when the SU transmits on the same channel as used by PU. For solving this problem, several methods are proposed to control, manage and avoid the interference. In general, the interference may be avoided by employing spectrum management, antenna directivity and power control.

Previously, some schemes have been suggested for interference avoidance in cognitive radio networks (CRNs). In [16], a primary receiver assisted interference avoidance (PRA-IA) strategy for CRN has been presented. For the interference avoidance, the scheme exploits the locations of the primary network which are underutilized. According to the reported simulation results, the throughput is enhanced as a result of interference avoidance. In [17], a fog computing aided spatial spectrum sharing mechanism with interference avoidance is proposed. Guard zone along with interference cancellation (GZ-IC) is used to provide spectrum access to SUs while restricting the secondary interference to the PUs. The work in [18] investigates optimal anti jamming power allocation in the cooperative CRN in the presence of

Manuscript received xxxxxxxxxx, 2021; revised xxxxxxxxxx, 2021, xxxxxxxxxx, 2022 and xxxxxxxxxx, 2022; accepted xxxxxxxxxx, 2022. Date of publication xxxxxxxxxx, 2022; date of current version xxxxxxxxxx, 2022. This work was supported in part by the Deanship of Scientific Research (DSR), King Abdulaziz University, Jeddah, under grant No. (G:265-611-1442). The authors, therefore, acknowledge with thanks DSR support. *(Corresponding author: Muhammad Farooq-i-Azam.)*

Muhammad Farooq-i-Azam is with Department of Electrical and Computer Engineering, COMSATS University Islamabad, Lahore Campus 54600, Pakistan. (e-mail: fazam@cuilahore.edu.pk).

Qiang Ni, Haris Pervaiz and Charilaos Zarakovitis are with School of Computing and Communications, Lancaster University, InfoLab21, LA1 4WA, U.K. (e-mail: q.ni@lancaster.ac.uk; h.b.pervaiz@lancaster.ac.uk; c.zarakovitis1@lancaster.ac.uk).

Mianxiong Dong is with Muroran Institute of Technology, Muroran 050-8585, Japan. (email: mx.dong@csse.muroran-it.ac.jp).

Fawaz Alsolami is with Department of Computer Science, King Abdulaziz University, Jeddah, Saudi Arabia. (email: falsolami1@kau.edu.sa).

Digital Object Identifier xxxx/xxxxxxxxxx

a smart jammer. The interaction between the CRN and the jammer is formulated as a Stackelberg game. By analyzing the optimal strategies for the CRN and the jammer, Stackelberg equilibrium of the game is derived. The Nash equilibrium is also derived for comparison with the Stackelberg equilibrium. Results show that the optimal power control strategies can minimize the jamming damage and help improve the CRN performance. The scheme proposed in [19] improves the sum rate of the secondary network and also guarantees the secrecy rate of the PU. In addition, principle of interference alignment is used for the elimination of interference at each SU and PU. The work in [20] proposes to use the secondary full duplex non orthogonal multiple access (NOMA) relay for secure primary transmission in cognitive radio networks. The primary transmitter transmits the primary signal to the relay, which generates artificial noise to prevent eavesdropping such that the primary transmission remains unaffected. Next, the relay transmits the superimposed signal to the primary and secondary receivers. Modified decoding order and joint beamforming optimization ensure security of the primary transmission. In [21], authors present a decision based framework in cognitive radio networks which includes different policies to decide which SUs can be dropped when a PU activity is sensed.

In this article, we extend our previous work [22] and use cooperative localization for the avoidance of interference. The distance between an SU and a PU is estimated by developing log normal shadowing path loss model of the interference link between them. The estimated distance is then leveraged to update the transmission power for the avoidance of interference. Simulation results reveal considerable performance gains due to the interference avoidance using the proposed scheme. The key motivations and contributions by this article are outlined in the following.

- Cooperation between the primary and the secondary networks is exploited for the avoidance of interference to facilitate effective spectrum utilization. A log normal shadowing model of the interference link between a PU and an SU is developed. This model is then further leveraged for cooperation between the primary and the secondary networks. In particular, the model is used for the distance estimation between a PU and an SU.
- A complete and robust cooperative localization model is presented. The model is used by a PU for the estimation of its position in cooperation with the neighbor SUs.
- The SUs transmit periodic beacon messages for the purpose of cooperative localization. A PU is able to estimate its position using the information provided by the beacon messages and the cooperative localization model. This position information is then used for an improved distance estimate between a PU and an SU.
- The distance information between the PU and the SU is used for the adjustment of the transmission power of the SU such that interference to the PU is avoided.
- A comprehensive set of simulation experiments is conducted to evaluate the performance of various aspects of the proposed method. In particular, performance with respect to distance and position estimation, channel availability, bandwidth utilization and channel capacity is investigated. The results reveal that the algorithm achieves considerable performance gains as a consequence of interference avoidance.

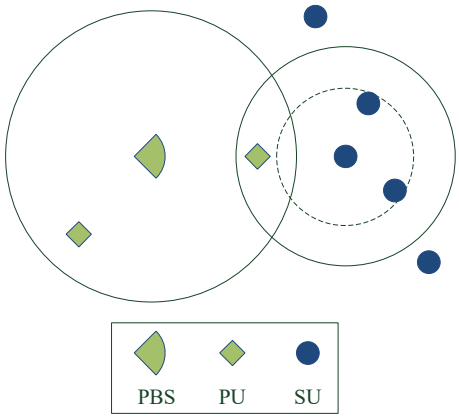

Fig. 1. System model.

The rest of this paper is organized as follows. The system model is presented in Section II. The position estimation by the PU using cooperative localization is discussed in Section III. In Section IV, the algorithm used for the interference avoidance is described. Simulation results are presented and discussed in Section V. Finally, the paper concludes with Section VI.

II. System Model

Let us consider a CRN deployed alongside an active primary radio network (PRN) as depicted in Fig 1. A PU is represented by p, where $p \in \mathbf{P} = \{1, 2, 3, ..., P\}$. Therefore, the set $\mathbf{P}$, of which p is a member, comprises of P number of PUs. In a similar manner, an arbitrary SU is represented using q, where $q \in \mathbf{Q} = \{1, 2, 3, ..., Q\}$. The number of SUs in the set $\mathbf{Q}$ is Q. We denote the transmission power of an SU q by P_{tq}, whereas its maximum permissible transmission power is represented by P_{max}. The transmission power of the primary base station (PBS) is represented using P_p. The maximum interference that is allowed at a PU p is termed as threshold of interference and is denoted by I_{pt}. The signal to interference noise ratio (SINR) at the PU p has a corresponding threshold value which is represented using β. The SINR γ_p of the transmission received by the PU p from the PBS should always be greater than β i.e. $\gamma_p > \beta$ in order to satisfy the interference constraint threshold I_{pt} and to avoid interference.

Let us now consider a scenario in which a PU p is situated in an area where its communication with the PBS is interfered by the transmissions of a nearby SU q. This is illustrated in Fig. 1. An interference channel exists between the SU q and the PU p due to the transmission of the former. The interference at PU p caused by the SU q should be minimized. This interference, denoted by I_p, is as below,

$$I_p = h_{qp} P_{tq}, \tag{1}$$

where h_{qp} represents the gain of the interference link between the PU p and the SU q. The SINR, γ_p at the PU p is obtained by using I_p from (1), as under,

$$\gamma_p = \frac{h_{pp}P_p}{I_p + BN_o}, \tag{2}$$

where B represents the channel bandwidth, N_o is the noise power spectral density (PSD), and h_{pp} denotes the gain of the PRN communication link between the PBS and the PU p. The threshold, I_{pt} of the interference, I_p allowable at a PU p so that the SINR γ_p remains above the threshold SINR β, can be obtained by substituting the threshold values, $I_p = I_{pt}$ and $\gamma_p = \beta$ in (2), as follows,

$$I_{pt} = \frac{1}{\beta}(h_{pp}P_p) - BN_o. \tag{3}$$

We use log normal distribution to model large scale fading to estimate path loss and shadowing. It is assumed that each SU in the CRN knows its location by the use of either an appropriate localization algorithm, such as, adaptive location estimation system [23] and ripple localization algorithm (RLA) [24], or a global navigation satellite system (GNSS).

Let us now determine the path loss suffered by the transmission of the SU q by the interference channel between the PU p and the SU q. This path loss, denoted by L_p, is obtained by using the log normal shadowing model, and is given by,

$$L_p[dB] = \overline{L}_{pa}(d_o) + 10\eta \log\left(\frac{d_{pq}}{d_o}\right) + \chi_\sigma, \tag{4}$$

where χ_σ accounts for the shadow fading, $\overline{L}_{pa}(d_o)$ is the average path loss at a reference distance d_o from the SU q, d_{pq} is the distance between the SU q and the PU p, and η is the path loss exponent. $\overline{L}_{pa}(d_o)$ is denoted by $\overline{L}_o$, if the reference distance d_o is the unit distance, and in this case,

$$L_p[dB] = \overline{L}_o + 10\eta \log(d_{pq}) + \chi_\sigma. \tag{5}$$

The PU p can use (5) to estimate the distance, d_{pq}, between itself and the SU q. This estimated distance is used for the transmission power adjustment of the SU for interference avoidance to the PU if distance estimates from no other SUs are available. On the other hand, if the PU has distance estimates from three or more SUs, then it can ascertain its position using cooperative localization as discussed in Section III. This position information can be used for ascertaining an improved estimate of the distance between the PU and the SU. The estimated distance can then be utilized for SU transmission power adjustment to avoid interference. We discuss and further explain this in Section IV. It is important to distinguish distance estimation from position estimation. The distance estimation is the estimation of Euclidean distance between two nodes. The position estimation, on the other hand, refers to the estimation of coordinates of a node. Moreover, the PRN is considered to be an active network so that the PUs may be transceivers which are able to transmit and receive messages.

III. Cooperative Localization

Each SU in the CRN knows its position information. A PU can also estimate its position with the assistance of SUs by cooperative localization. For this purpose, a beacon message, as shown in Fig. 2, is transmitted by each SU. In this beacon message, t_s denotes the time stamp, (x_q, y_q) represents the SU q position, and P_{tq} stands for the transmission power. When the beacon message is received, the PU determines the received signal strength (RSS) which is then used for the estimation of the path loss and hence, the distance as discussed in Section IV.

The SUs transmit periodic beacon messages except when the CRN is inactive and there is no interference. Hence, beacon messages from more than one SU may be received by the PU p. In case, beacon messages from three or more SUs are received by the PU, the distances from all these SUs are estimated by the PU. The beacon messages from these SUs include their respective positions. Therefore, the PU can perform multilateration with the knowledge of the positions of the SUs and the distances estimated from them. Next, the PU transmits a unicast message to the SU after estimating its position. In the PU message, which is shown in Fig. 3, t_p represents the time stamp, d_{pq} denotes the distance estimated using the RSS information, and (x, y) is the position estimated by the PU p using multilateration. It is to be noted that the exchange of messages between the SUs and the PUs is in a manner to provide real time performance. It is further to be noted that the proposed algorithm is cooperative in nature. Therefore, cooperation and sharing of information between SUs and PUs, as given in Fig. 2 and Fig. 3, is required for the algorithm to work. Primary user cooperation with the secondary network is not a new idea and has been explored in earlier work as well, for example, [16] and [25]. However, the PUs share the information only in unicast messages. Therefore, the information is shared only with a limited number of nodes. As a result of the cooperative exchange, the PUs are able to estimate their positions. It is to be noted that the proposed method requires that the PU is able to transmit

SID	t_s	(x_q, y_q)	P_{tq}

SID – SU node identification
t_s – Time stamp by SU
(x_q, y_q) – Position coordinates of SU
P_{tq} – SU transmission power

Fig. 2. Beacon message transmitted by SU.

PID	t_p	L_p	d_{pq}	(x, y)

PID – PU node identification
t_p – Time stamp by PU
L_p – Measured path loss
d_{pq} – Estimated distance
(x, y) – Estimated position

Fig. 3. Message transmitted by PU.

unicast messages. Therefore, it can be deployed only with those primary networks where the PU is a transceiver.

Let us consider that the PU p receives beacon messages from n number of SUs for a further explanation of the position estimation procedure. The PU is able to determine the positions of these SUs from the beacon messages, and are given by (x_1, y_1), (x_2, y_2), ..., (x_q, y_q), ..., (x_n, y_n). Let the distances from these SUs are estimated to be r_1, r_2, ..., r_q, ..., r_n respectively. If we denote the position information of the PU p by (x, y), then considering the positions of the SUs as centers and their respective distance estimates r_1, r_2, ... r_n from the PU p as radii, the following set of equations of circles around the SUs are obtained,

$$\begin{bmatrix} (x-x_1)^2+(y-y_1)^2 \\ (x-x_2)^2+(y-y_2)^2 \\ \vdots \\ (x-x_n)^2+(y-y_n)^2 \end{bmatrix} = \begin{bmatrix} r_1^2 \\ r_2^2 \\ \vdots \\ r_n^2 \end{bmatrix}. \tag{6}$$

Expanding square terms on the left side and rearranging:

$$\begin{bmatrix} x^2+y^2-2x_1x-2y_1y \\ x^2+y^2-2x_2x-2y_2y \\ \vdots \\ x^2+y^2-2x_nx-2y_ny \end{bmatrix} = \begin{bmatrix} r_1^2-x_1^2-y_1^2 \\ r_2^2-x_2^2-y_2^2 \\ \vdots \\ r_n^2-x_n^2-y_n^2 \end{bmatrix}. \tag{7}$$

Subtracting last row from each of the rows above it:

$$\begin{bmatrix} 2(x_n-x_1)x+2(y_n-y_1)y \\ 2(x_n-x_2)x+2(y_n-y_2)y \\ \vdots \\ 2(x_n-x_{n-1})x+2(y_n-y_{n-1})y \end{bmatrix} = \begin{bmatrix} r_1^2-r_n^2+x_n^2-x_1^2+y_n^2-y_1^2 \\ r_2^2-r_n^2+x_n^2-x_2^2+y_n^2-y_2^2 \\ \vdots \\ r_{n-1}^2-r_n^2+x_n^2-x_{n-1}^2+y_n^2-y_{n-1}^2 \end{bmatrix}. \tag{8}$$

Separating the unknowns (x, y), this can be rewritten as below:

$$\begin{bmatrix} (x_n-x_1) & (y_n-y_1) \\ (x_n-x_2) & (y_n-y_2) \\ \vdots & \vdots \\ (x_n-x_{n-1}) & (y_n-y_{n-1}) \end{bmatrix} \begin{bmatrix} x \\ y \end{bmatrix} = \frac{1}{2} \begin{bmatrix} r_1^2-r_n^2+x_n^2-x_1^2+y_n^2-y_1^2 \\ r_2^2-r_n^2+x_n^2-x_2^2+y_n^2-y_2^2 \\ \vdots \\ r_{n-1}^2-r_n^2+x_n^2-x_{n-1}^2+y_n^2-y_{n-1}^2 \end{bmatrix}. \tag{9}$$

Using matrix notation, this can be written as:

$$\mathbf{Az} = \mathbf{R}, \tag{10}$$

where $\mathbf{z} = \begin{bmatrix} x & y \end{bmatrix}^T$ and

$$\mathbf{A} = \begin{bmatrix} (x_n-x_1) & (y_n-y_1) \\ (x_n-x_2) & (y_n-y_2) \\ \vdots & \vdots \\ (x_n-x_{n-1}) & (y_n-y_{n-1}) \end{bmatrix}, \tag{11}$$

$$\mathbf{R} = \frac{1}{2} \begin{bmatrix} r_1^2-r_n^2+x_n^2-x_1^2+y_n^2-y_1^2 \\ r_2^2-r_n^2+x_n^2-x_2^2+y_n^2-y_2^2 \\ \vdots \\ r_{n-1}^2-r_n^2+x_n^2-x_{n-1}^2+y_n^2-y_{n-1}^2 \end{bmatrix}. \tag{12}$$

To find the position of the PU p, which we represent by (x, y), let us formulate (6) as a least squares problem as below:

$$\hat{z} = \underset{z}{\operatorname{argmin}} \sum_{i=1}^{n} e_i(z)^2, \tag{13}$$

where $\mathbf{z} = \begin{bmatrix} x & y \end{bmatrix}^T$ is the best-fit estimated position, $e_i(z)$ is the residual function, and is expressed as,

$$e_i(z) = r_i^2 - \{(x-x_i)^2 + (y-y_i)^2\}, \tag{14}$$

where $i = 1, 2, ..., n$. The formulation of the problem in (13), which is based upon (6), is nonlinear least squares. Specifically, it is unconstrained nonlinear optimization problem. The problem is reduced to linear least squares in (9). We can formulate the least squares approximation based upon (9), as under,

$$\hat{z} = \underset{z}{\operatorname{argmin}} \sum_{i=1}^{n-1} e_i(z)^2. \tag{15}$$

In this case, the residual function can be written as,

$$e_i(z) = b_i - \{a_{i1}x + a_{i2}y\} \tag{16}$$

where

$$a_{i1} = x_n - x_i, \tag{17}$$

$$a_{i2} = y_n - y_i, \tag{18}$$

$$b_i = \frac{1}{2}\{r_i^2 - r_n^2 + x_n^2 - x_i^2 + y_n^2 - y_i^2\} \tag{19}$$

and $i = 1, 2, ..., n-1$. We can write the sum of the squared residuals, S, as below,

$$S = \sum_{i=1}^{n-1} e_i^2 = \sum_{i=1}^{n-1} \{b_i - (a_{i1}x + a_{i2}y)\}^2. \tag{20}$$

The objective is to find the minimum of the function in (20). The position coordinates, (x, y), for which the sum of the squares of the residuals, S is the minimum, are evaluated as under,

$$\frac{\partial S}{\partial x} = 0, \tag{21}$$

$$\frac{\partial S}{\partial y} = 0. \tag{22}$$

Differentiating (20) with respect to x and equating the result to 0, we obtain,

$$\sum_{i=1}^{n-1} (a_{i1}x + a_{i2}y)a_{i1} = \sum_{i=1}^{n-1} a_{i1}b_i. \tag{23}$$

Differentiating (20) with respect to y and equating the result to 0, we obtain,

$$\sum_{i=1}^{n-1} (a_{i1}x + a_{i2}y)(a_{i2}) = \sum_{i=1}^{n-1} a_{i2}b_i, \tag{24}$$

We combine (23) and (24) in the matrix form to obtain the following normal equation,

$$\mathbf{A^T A z} = \mathbf{A^T R}. \tag{25}$$

After subtracting the last row from the rows the other rows, the order of matrix $\mathbf{A}$ in (9)-(11) is $(\mathbf{n-1}) \times \mathbf{2}$. As matrix $\mathbf{A}$ is not necessarily square, we cannot use

$$\mathbf{z} = \mathbf{A^{-1} R}, \tag{26}$$

to determine $\mathbf{z}$. However, we can represent (25) in simplified form as below:

$$\mathbf{Hz} = \mathbf{T}, \tag{27}$$

where $\mathbf{H} = \mathbf{A^T A}$ and $\mathbf{T} = \mathbf{A^T R}$. As noted earlier, the matrix $\mathbf{A}$ has an order of $(n-1) \times 2$. Therefore, the order of matrix $\mathbf{A^T}$ is $2 \times (n-1)$. Consequently, the order of the resultant matrix $\mathbf{H} = \mathbf{A^T A}$ is 2×2. Therefore, (27) is, in fact, a combination of linear equations. Using ordinary techniques, we can solve this system of equations to find $\mathbf{z} = \begin{bmatrix} x & y \end{bmatrix}^T$. It is to be noted that we choose to estimate the position of the PU only when it receives beacon messages from at least three different SUs. As a result, $n - 1 \geq 2$ i.e. the number of rows in the matrix $\mathbf{A}$ is always equal to or greater than the number of columns, which is always two. This also ensures that the number of rows in the matrix $\mathbf{A}$ is at least two so that a solution for the two unknown values, x and y, is feasible. As the matrix elements are derived from the independent and random positions of SUs, the rows and columns are linearly independent and the matrix $\mathbf{A}$ is full rank. As a result, the matrix $\mathbf{A}$ is nonsingular and invertible and the achieved solution in (27) is unique. This gives us an exact solution if it exists and an approximate solution otherwise.

IV. Interference Avoidance

We describe the proposed interference avoidance algorithm in this section. One part of the algorithm is executed by the SU q and the other part is executed by the PU p.

An information beacon message, as depicted in Fig. 2, is transmitted by each SU periodically. The PU p measures the RSS when the beacon message is received. The path loss can then be calculated using the RSS information. Let the RSS of the SU q transmitted interference signal at the PU p be represented by P_{qp}. The path loss is then given by,

$$L_p[dB] = P_{tq}[dB] - P_{qp}[dB]. \tag{28}$$

After estimating the path loss with the help of RSS information and (28), the distance is also ascertained as under,

$$\log(d_{pq}) = \frac{1}{10\eta}\Big[L_p[dB] - \overline{L}_o - \chi_\sigma\Big], \tag{29}$$

$$d_{pq} = 10^{\frac{1}{10\eta}\left[L_p[dB] - \overline{L}_o - \chi_\sigma\right]}. \tag{30}$$

The PU p estimates this distance, d_{pq}, using the RSS value. The distance between the SU q and the PU p can also be estimated using their respective location information. As stated earlier, each SU already knows its location using GNSS or a localization algorithm. Furthermore, as already discussed in Section III, the PU p can also estimate its position using cooperative localization. If beacon messages are received from at least three SUs by the PU p, then the position can be ascertained. For this, the distances from all these SUs are estimated. The PU also knows the positions of these SUs from their received beacon messages. Using the position and distance information of these SUs, the PU uses a formulation similar to (6), which is solved using (27) for the estimation of the position (x, y) of the PU. On the other hand, if the number of received beacon messages is less than three and the position cannot be ascertained by the PU p, then an absurd value, say, $(-1, -1)$ is assigned to (x, y) to inform the SU about unavailability of its position information. Therefore, the SU then uses the distance estimate d_{pq} for power control.

The PU p sends a message as shown in Fig. 3, after it has estimated the distance d_{pq} and determined its position (x, y). When the SU q receives a PU message, it examines it for a valid location detail of the PU. Given that the PU message carries a valid position information, the SU q uses its own position and the received information to estimate the distance, d_{xy}, between itself and the PU p.

$$d_{xy} = \sqrt{(x_q - x)^2 + (y_q - y)^2}. \tag{31}$$

If the PU p is able to estimate its position as a consequence of receiving beacon messages from at least three SUs, then two different estimates of the distance between the PU p and SU q are available to the SU. The first estimate is the distance d_{pq}, which is found using the RSS value by the PU, and the second estimate is denoted by d_{xy}, which is calculated from the location information of the SU and the PU. In the case, when the PU p is not able to estimate its position because it did not receive beacon messages from at least three SUs, then d_{xy} cannot be calculated and only one distance estimate, d_{pq}, is available to the SU. The distance estimate d_{xy} is preferred by the SU when both the distance estimates are available. The distance d_{xy} has lesser chance of error [24], as information from at least three SUs is used for its estimation.

The SU q is able to confirm whether the PU p is inside its communication range R with the help of the distance detail. After the SU q confirms this, it revises its transmission power, in such a manner, that $P_{qp} < I_{pt}$, by a factor θ, which we call as the reduction factor and $0 < \theta < 1$.

$$P_{qp} = (1 - \theta) I_{pt}, \quad 0 < \theta < 1. \tag{32}$$

The updated transmission power, P_{tqn}, is then as below,

$$P_{tqn}[dB] = L_p[dB] + (1 - \theta) I_{pt}[dB], \tag{33}$$

where L_p represents the path attenuation estimated by the PU p with the help of the RSS details.

The transmission power updated in this manner should yield a new value which is smaller than the transmission power used previously. Nonetheless, a wrong estimate of the path attenuation may lead to an incorrect estimate of the new value of transmission power. Consequently, the new updated transmission power may be greater than the previous value. If this is the case and $P_{tqn} > P_{tq}$, then this is ascribed to the shadowing in the interference channel. That being so,

the estimated path attenuation is greater than the attenuation when there is no fading. Consequently, the RSS is lower, and hence the distance estimate is higher than the actual distance. Therefore, when P_{tqn} determined using the path loss information is found to be greater than the previously used value, then the shadowing model is updated, and the path loss calculation is performed as below,

$$L_p[dB] = \overline{L}_o + 10\eta \log(d) + \chi_\sigma, \tag{34}$$

where d is d_{xy} if available and d_{pq} otherwise. After this, the transmission power is revised using the value of the path loss calculated using (34) instead of the measured value in (28) until $P_{tqn} < P_{tq}$ and the corresponding new transmission range R becomes smaller than the distance separating the SU q and the PU p.

The exchange of a pair of messages between the PU p and the SU q should result in the avoidance of interference. However, the procedure may have to be repeated in the presence of shadow fading. In the latter case, the SU q transmits a periodic beacon message. In response, the PU p replies with a response message, and the SU q again updates its transmission power. The procedure is repeated until the interference is below the threshold level, and no more messages can be exchanged between the PU p and SU q. The algorithms executed by the PU p and SU q are summarized in Algorithm 1 and Algorithm 2 respectively.

It is to be noted that an SU may estimate and keep a record of its transmission range using experimental calibration for various power levels or by using:

$$R = 10^{\frac{1}{10\eta}\left[L_{pmax}[dB] - \overline{L}_o - \chi_\sigma\right]}, \tag{35}$$

where L_{pmax} is the maximum path loss, which can be estimated as following:

$$L_{pmax} = P_{tq} + G_t + G_r - S_i - F, \tag{36}$$

where G_t and G_r are gains of the transmitting and receiving antennas respectively, S_i is the receiver sensitivity and F is the fade margin. All these parameters are specified in dB.

Algorithm 1 The Primary User

procedure POSITIONESTIMATION( )
  Receive beacon message
  t_s, (x_q, y_q), $P_{tq} \leftarrow$ Beacon message
  $P_{qp} \leftarrow RSS$
  $L_p[dB] \leftarrow P_{tq}[dB] - P_{qp}[dB]$
  $d_{pq} \leftarrow 10^{\frac{1}{10\eta}\left[L_p[dB] - \overline{L}_o - \chi_\sigma\right]}$
  if $(n \geq 3)$ **then**
    Formulate $\mathbf{Az} = \mathbf{R}$
    Derive $\mathbf{Hz} = \mathbf{T}$
    Determine $\mathbf{z}$ from $\mathbf{Hz} = \mathbf{T}$
    $(x, y) \leftarrow \mathbf{z}$
  else
    $(x, y) \leftarrow (-1, -1)$
  end if
  PU message $\leftarrow L_p$, d_{pq}, (x, y)
  Transmit PU message
end procedure

Algorithm 2 The Secondary User

procedure TRANSMITPOWER( )
  Transmit beacon message
  Receive PU message
  L_p, d_{pq}, $(x, y) \leftarrow$ PU message
  if $(x, y) \neq (-1, -1)$ **then**
    $d_{xy} \leftarrow \sqrt{(x_q - x)^2 + (y_q - y)^2}$
    $d \leftarrow d_{xy}$
  else
    $d_{xy} \leftarrow -1$
    $d \leftarrow d_{pq}$
  end if
  if $(d \leq R)$ **then**
    $P_{tqn}[dB] \leftarrow L_p[dB] + (1 - \theta)I_{pt}[dB]$
  end if
  if $(P_{tqn} \geq P_{tq})$ **then**
    while $(P_{tqn} \geq P_{tq})$ **and** $(d \leq R)$ **do**
      $\sigma \leftarrow \sigma - 1$
      $L_p[dB] \leftarrow \overline{L}_o + 10\eta \log(d) + \chi_\sigma$
      $P_{tqn}[dB] \leftarrow L_p[dB] + (1 - \theta)I_{pt}[dB]$
      $R \leftarrow 10^{\frac{1}{10\eta}\left[L_{pmax}[dB] - \overline{L}_o - \chi_\sigma\right]}$
    end while
  end if
end procedure

V. SIMULATION RESULTS

For our evaluation using simulation, a CRN with a 500 m radius is considered. The number of SUs in the CRN is 5 unless otherwise stated. The maximum transmission power of an SU is 23 dBm, and the minimum transmission power is assumed to be -33 dBm. Furthermore, it is presumed that the SUs update their location periodically. The number of PUs is considered to be 2. The bandwidth of each subchannel is 0.3125 MHz [26]. The bandwidth of the interference channel is assumed to be the same as that of the PU. The path loss exponent η is assumed to be 2 to 4. Noise power, N_o is considered to be 3×10^{-15} W/Hz. Shadow fading standard deviation σ is 6 dB. It is presumed that the interference threshold I_{pt} of a PU is 5×10^{-12} W [26]. The beacon transmission interval is configured to be 102.4 ms, and beacon frame collisions are avoided using time synchronization. In the cooperative set up, the beacon frames are transmitted on agreed up control channel. Therefore, this does not result in any interference to the PUs. The simulation parameters are summarized in Table I. These parameters are representative of a typical wireless communication network [27]. Similar parameters are also used by related work in this area, such as [26] and [28].

In Fig. 4, we plot the distance estimated by the PU, d_{pq}, against the received power. It is plotted versus the path loss in Fig. 5. From the plots, it can be seen that a low value of received power implies a large estimated distance between the SU and the PU. On the contrary, an increase in the path loss results in a relatively higher estimate of the distance. In particular, beyond a distance of 85 m, the path

TABLE I
SIMULATION PARAMETERS.

Parameter	Value
Number of SUs	5
Number of PUs	2
Minimum transmission power of SU	-33 dBm
Maximum transmission power of SU	23 dBm
Center frequency	500 MHz
Channel bandwidth	0.3125 MHz
Path loss exponent	2 to 4
Shadow fading standard deviation	6 dB
Noise power	3×10^{-15} W/Hz
PU interference threshold	5×10^{-12} W
Beacon transmission interval	102.4 ms

loss increases very quickly. Conversely, a rise in the path attenuation up to 60 dB implies only a slight increment in the distance estimation. Beyond this point, however, only a slight increment in the path attenuation implies a substantial increment in the estimated distance. For example, for an increase in the path attenuation from 40 to 60 dB, the increase in the estimated distance is from 40 to 85 m approximately. This is a variation of approximately 40 m per 20 dB. On the other hand, the distance estimate changes from 200 to 400 m with an increment in the path attenuation from 80 to 100 dB. This implies a variation of 200 m per 20 dB. The results observed from Fig. 4 are similar. When the received power is small, the slope is high. However, for large values of the received power, there is a gradual and gentle decline in the slope. A steep decline in the slope with large path loss and small values of the received power can be ascribed to the densely populated urban environment which results in a high path loss exponent.

The distance d_{pq} as plotted in Fig. 4 and Fig. 5 is estimated by the PU between itself and the SU. Moreover, the same distance is also estimated by the SU using the position information, and is represented by d_{xy}. The distance estimation error, which is defined as the absolute difference between the estimated and the actual distances, is plotted for both d_{pq} and d_{xy} in Fig. 6 and Fig. 7. The distance estimation error is plotted against the average received power in Fig. 6 and versus the average path loss in Fig. 7. As can be seen from the plots in Fig. 6 and Fig. 7, the distance estimation error is high when the average received power is small or when the average path loss is high. These results are in conformance with the results plotted in Fig. 4 and Fig. 5. It was observed from Fig. 5 that the slope is small for the small values of the path loss while it is high for the large values. Therefore, a small inaccuracy in the path attenuation is reflected as a large error in the distance estimate when the path attenuation is high. Likewise, a small inaccuracy in the value of the received power results in a large value of the distance estimation error when the received power is small. In either case, it is at the long distances that the distance estimation error is high. For small distances, the accuracy of distance estimation is relatively better and the distance estimation error is small. It is further observed that the distance estimation error is comparatively smaller for d_{xy} compared to that for d_{pq}. This can be attributed to a better estimate of d_{xy} using position coordinates. The actual position of the SU is known and only position of PU is estimated using trilateration with three or more nodes. Therefore, the error in the estimation is small. From the plots, it is also seen that the difference in the distance

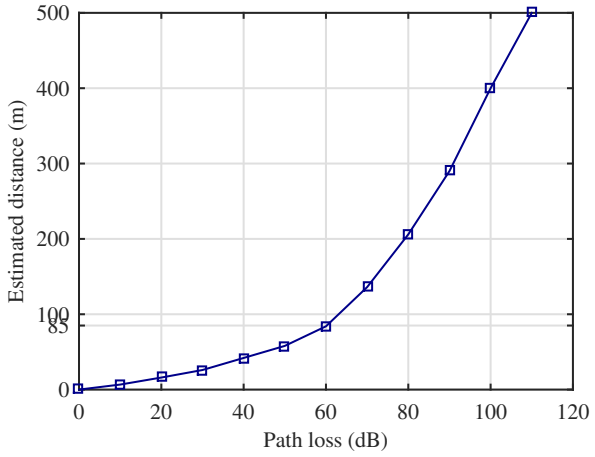

Fig. 5. Change in the distance estimate with the path loss.

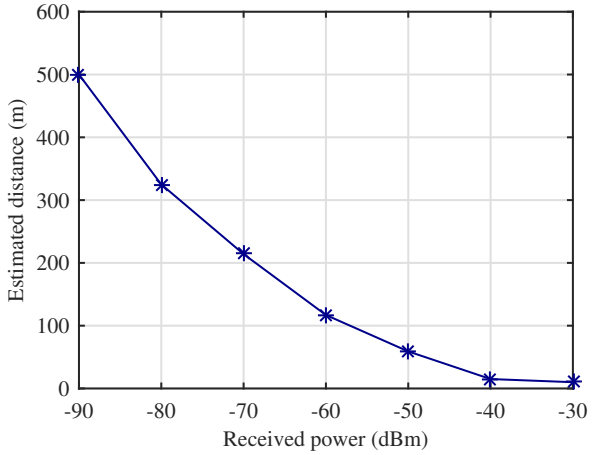

Fig. 4. Estimated distance versus the received power.

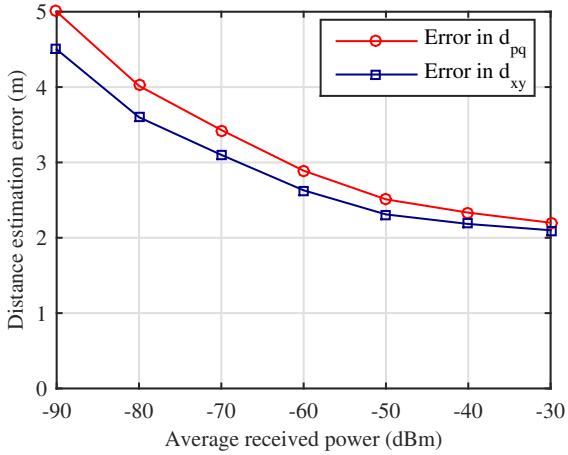

Fig. 6. Distance estimation error versus average received power.

estimation errors for d_{xy} and d_{pq} is high at those points where the slope of the curve is steep. Again, this is due to a large value of the distance estimation error induced by a relatively smaller inaccuracy in the estimation of path attenuation and the received power.

The distance estimation error is plotted against the average SINR also in Fig. 8. At relatively closer distances, the received SINR is large as the path loss is small. Therefore, with the change in the distance with the movement of the object, the relative change in the SINR with respect to the received large SINR is also small. Hence, small variations in the SINR do not significantly affect the distance estimation error at close distances. At long distances, the received SINR is comparatively small, and therefore, even a little variation in the SINR is significant as it may result in noticeable change in the received SINR. Even movement of objects in the vicinity of the user may result in momentary fading, which results in fluctuations in the SINR. As a result, a small variation in the SINR translates to a large distance estimation error when the receiver is at a long distance from the transmitter. Hence, the plot in Fig. 8 corroborates the results in Fig. 6 and Fig. 7.

Error in the distance estimation leads to localization error when the PU estimates its position with the help of position information of known SUs and the distances estimated from them. The localization error is plotted in Fig. 9 against the number of SUs used for the estimation of the position. It is plotted in Fig. 10 versus the average received power from the SUs, and against the path loss in Fig. 11. It is observed from Fig. 9 that the localization error decreases as the number of reference SUs is increased for position estimation by the PU. This can be attributed to multilateration where position estimation with a large number of reference nodes results in the reduction of localization error [24]. It is observed from Fig. 10 that the localization error is large when the received power is low. Similarly, from Fig. 11 it can be seen that the localization error is high when the path loss is high. This happens when the distance between the PU and the SU is large, and as a result, the path loss is large and the received signal strength is low. Consequently, any slight change in the received signal strength is significant due to its low value and results in large distance estimation error as discussed in the previous paragraphs in this section. The large distance estimation error results in large localization error. To further elaborate this, let us denote the received power at a particular distance d by P and the change in the received power at a distance $d + \Delta d$ by ΔP. At closer distances, ΔP is small and P is large. At longer

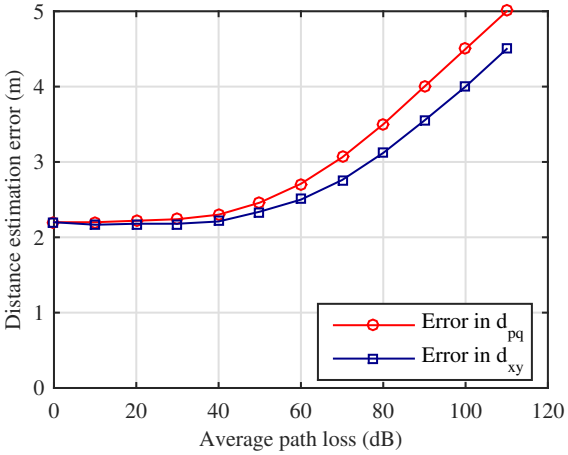

Fig. 7. Distance estimation error versus the average path loss.

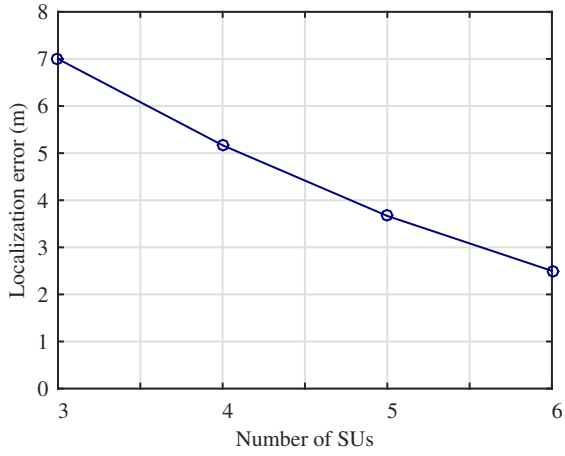

Fig. 9. Change in localization error with the the number of SUs.

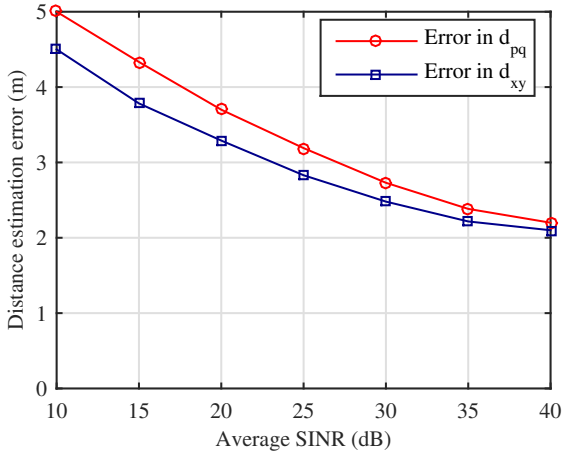

Fig. 8. Distance estimation error versus the average SINR.

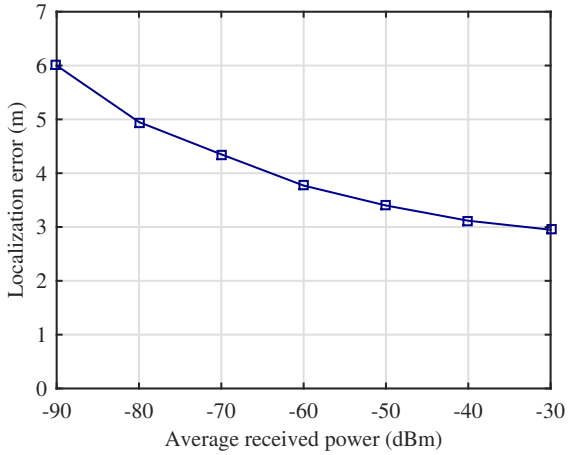

Fig. 10. Localization error versus average received power.

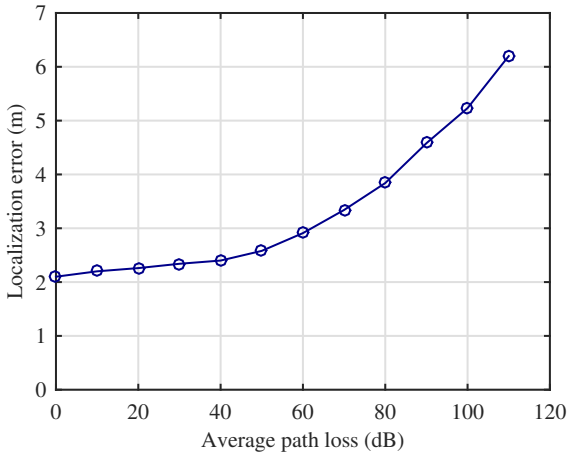

Fig. 11. Variation in localization error with average path loss.

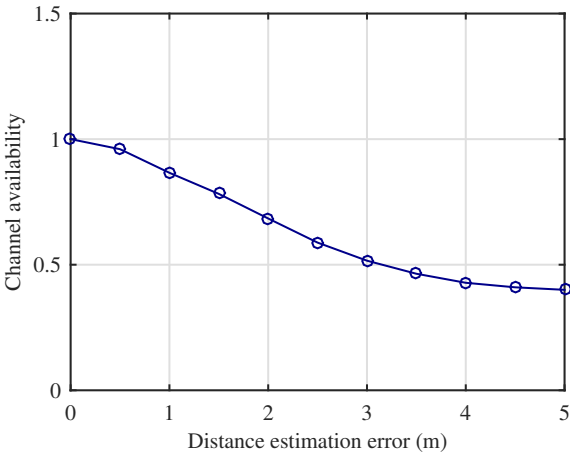

Fig. 12. Channel availability versus distance estimation error.

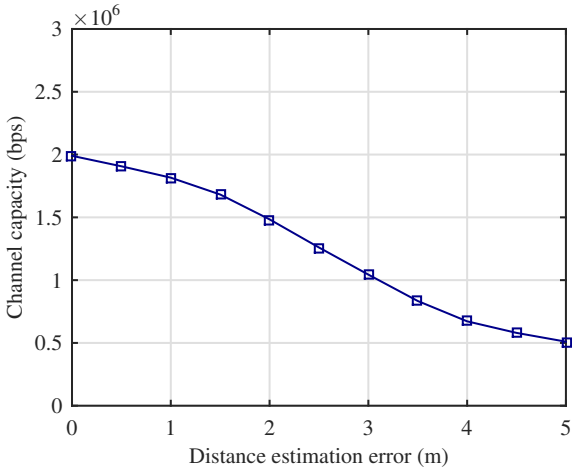

Fig. 13. Effect of the negative distance estimation error on the channel capacity for secondary users.

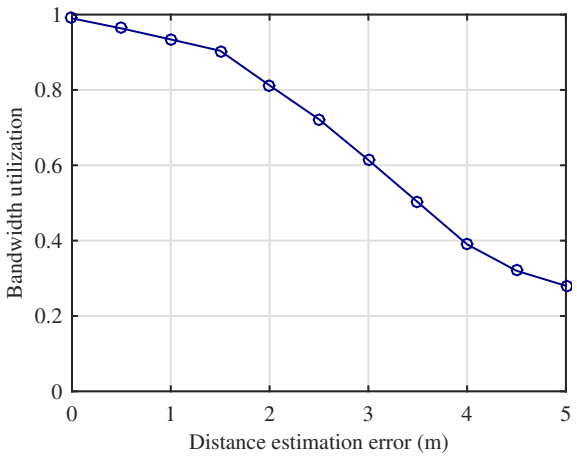

Fig. 14. Bandwidth utilization with the change in distance estimation error.

distances, ΔP is large and P is small. As a result, the distance estimation resolution which is inversely proportional to $\frac{\Delta P}{\Delta d}$ is high at close distances and small at long distances. Therefore, distance estimates at close distances are better than those at relatively longer distances. Consequently, the localization error is relatively higher at long distances than at the close distances.

Channel availability is plotted versus distance estimation error in Fig. 12. As can be observed, the channel availability decreases with the increase in the distance estimation error. The SU may estimate the PU to be within its transmission range due to the distance estimation error. As a result, it does not utilize the channel even though it may not be occupied. This results in lowering of the channel availability with the increase in the error in the distance estimate.

As the transmission power is updated based on the estimated distance, an error in the distance estimation has an impact on SINR and the channel capacity. The distance estimation error can be either positive or negative. A positive distance estimation error implies that the estimated distance is greater than the actual distance whereas a negative distance estimation error means that the estimated distance is smaller than the actual distance. A positive distance estimation error will result in the allocation of higher transmission power than the required and a negative distance estimation error will result in transmission power allocation which is lower than the value needed for interference avoidance. The former case may require more than one iteration in Algorithm 2 for interference avoidance whereas the latter situation results not only in interference avoidance in the first instance but may also degrade channel capacity for the SU. The degradation in channel capacity for SU with negative distance estimation error is plotted in Fig. 13. A high value of negative distance estimation error results in the allocation of transmission power which is lower than that would have been sufficient for interference avoidance. This achieves the desired result of interference avoidance. However, the SINR at the receiver also becomes smaller than the desired value. This eventually results in lowering of the capacity.

Distance estimation error has adverse effect on the bandwidth utilization as well. This is reported in the result plotted in Fig. 14. The plot is similar to that in Fig. 13. Distance estimation error results in inaccurate estimate of the boundary of the transmission of SU, and as a result the SU may reduce its transmission power considering the PU to be within its range. This will protect the PU transmissions but will

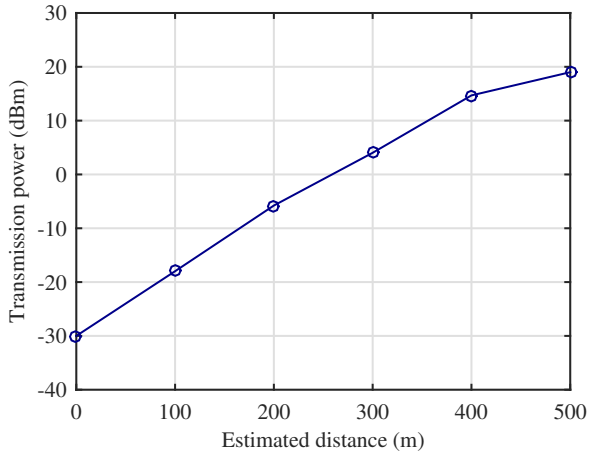

Fig. 15. Transmission power allocation versus the estimated distance.

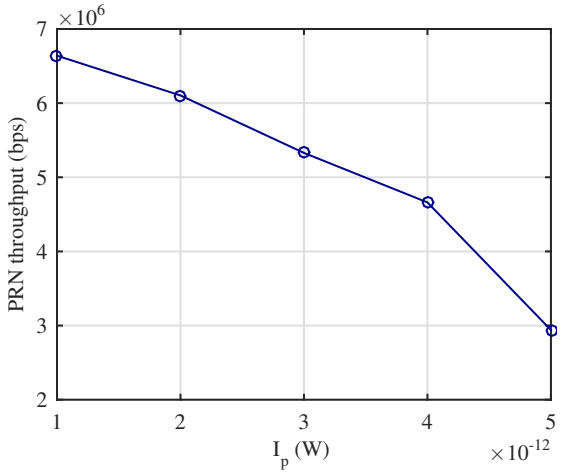

Fig. 17. PRN throughput with the variation in I_p.

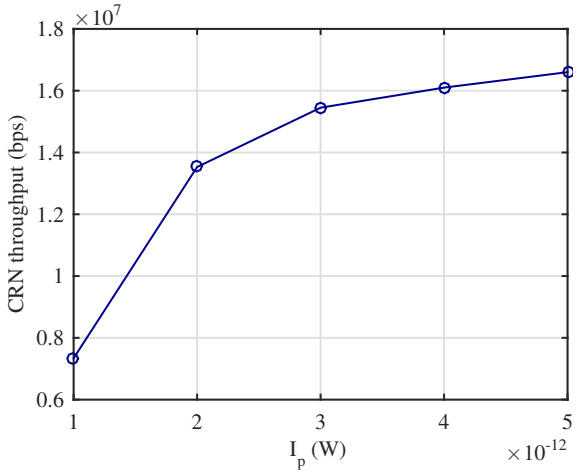

Fig. 16. CRN throughput with the variation in I_p.

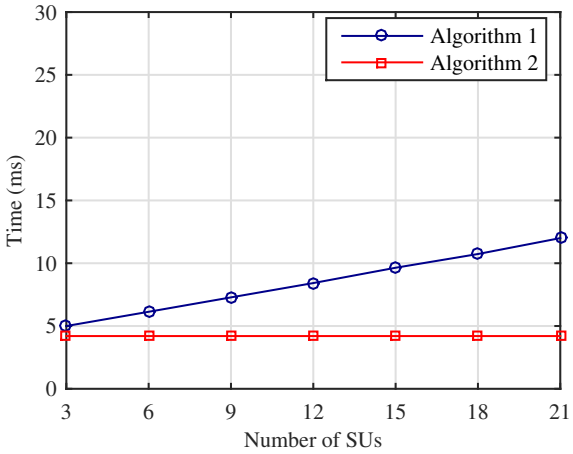

Fig. 18. Time required by the algorithm for different number of SUs.

have adverse effect on the bandwidth utilization of the channel between the SU transmitter and SU receiver. High frequency components and harmonics of the transmitted signal with small amplitude will suffer greater path loss and attenuation. Due to the attenuation of the high frequency signal components, the signal bandwidth is reduced and, as a result, the available channel bandwidth is not fully utilized.

The transmission power allocation as a function of the estimated distance using the proposed algorithm is plotted in Fig. 15. As expected, the higher the distance, the higher the allocated transmission power. The CRN and the PRN throughputs versus the interference at the PU resulting from the SU transmission are plotted in Fig. 16 and Fig. 17 respectively. With the increase in the SU transmission power, the CRN throughput increases although the interference at the PU also increases as is shown in Fig. 16. On the other hand, the PRN throughput decreases with this increase in the interference at the PU as is depicted in Fig. 17.

The time required by the algorithm for different number of SUs is plotted in Fig. 18. For Algorithm 1, the time increases with the number of SUs. As the number of SUs increases, the PU has to process a higher number of position coordinates for the estimation of the position. Therefore, the time increases with the number of SUs from which the PU receives beacon messages. However, the time required by Algorithm 2 remains the same as it is independent of the number of SUs.

Throughput of the secondary network against SINR using the proposed method is compared with the throughput obtained using two other existing schemes i.e. GZ-IC [16], and PRA-IA [17]. The results are plotted in Fig. 19. It can be observed that GZ-IC provides good results at small values of SINR. However, overall performance of the proposed method is better than the other two schemes.

We have evaluated the performance of the proposed algorithm from various aspects. For example, we have evaluated distance estimation, localization error, channel availability, channel capacity and bandwidth utilization for the proposed interference avoidance scheme. The results give considerable insight into the performance of the proposed method. We can infer that the proposed scheme provides distance estimation based interference avoidance and its performance is correlated with the accuracy of the distance estimation. Performance of the network improves as a result of the interference avoidance using the proposed algorithm.

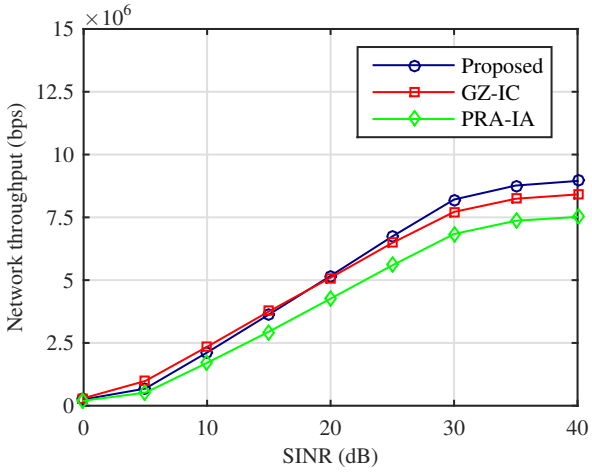

Fig. 19. Comparison of the throughput of the secondary network using the proposed method, GZ-IC and PRA-IA.

VI. Conclusion

In this paper, primary user assisted localization has been exploited to avoid interference. The localization along with path loss model is used to estimate the distance between the primary and secondary users. After the distance is estimated, secondary user transmission power adjustment is used for interference avoidance to the primary user. Different aspects of the proposed scheme are evaluated using simulation experiments. Estimated distance, distance estimation error and localization error are measured against path loss, received power and SINR. Similarly, performance of the proposed method with respect to channel availability and channel capacity is also evaluated. From the results, it is evident that the performance improves due to interference avoidance using the proposed method. We find that the achieved performance is, however, a function of the distance estimation error. The improvement in throughput and bandwidth utilization decreases with the increase in the distance estimation error, and increases when the distance estimation error is small.

References

[1] A. Hu and J. He, "Position-aided beam learning for initial access in mmWave MIMO cellular networks," *IEEE Systems Journal*, pp. 1–11, 2020.

[2] Y. Shi, E. Alsusa, and M. W. Baidas, "Energy-efficient decoupled access scheme for cellular-enabled UAV communication systems," *IEEE Systems Journal*, pp. 1–12, 2021.

[3] Y. Su, X. Lu, Y. Zhao, L. Huang, and X. Du, "Cooperative communications with relay selection based on deep reinforcement learning in wireless sensor networks," *IEEE Sensors Journal*, vol. 19, no. 20, pp. 9561–9569, 2019.

[4] S. Hriez, S. Almajali, H. Elgala, M. Ayyash, and H. B. Salameh, "A novel trust-aware and energy-aware clustering method that uses stochastic fractal search in IoT-enabled wireless sensor networks," *IEEE Systems Journal*, pp. 1–12, 2021.

[5] G. Hattab and D. Cabric, "Energy-efficient massive IoT shared spectrum access over UAV-enabled cellular networks," *IEEE Transactions on Communications*, vol. 68, no. 9, pp. 5633–5648, 2020.

[6] J. Li, X. Li, J. Yuan, Y. Gao, and R. Zhang, "An energy-constrained forwarding scheme based on group trustworthiness in mobile internet of things," *IEEE Systems Journal*, pp. 1–12, 2021.

[7] F. Bouhafs, M. Seyedebrahimi, A. Raschellà, M. Mackay, and Q. Shi, "Per-flow radio resource management to mitigate interference in dense IEEE 802.11 wireless LANs," *IEEE Transactions on Mobile Computing*, vol. 19, no. 5, pp. 1170–1183, 2020.

[8] P. Liu, Q. Hu, K. Jin, G. Yu, and Z. Tang, "Toward the energy-saving optimization of WLAN deployment in real 3-D environment: A hybrid swarm intelligent method," *IEEE Systems Journal*, pp. 1–12, 2021.

[9] W. Stallings, *Wireless Communications & Networks*. Pearson Education, 2009.

[10] A. Memedi and F. Dressler, "Vehicular visible light communications: A survey," *IEEE Communications Surveys Tutorials*, pp. 1–1, 2020.

[11] H. Elayan, O. Amin, B. Shihada, R. M. Shubair, and M. Alouini, "Terahertz band: The last piece of RF spectrum puzzle for communication systems," *IEEE Open Journal of the Communications Society*, vol. 1, pp. 1–32, 2020.

[12] S. Muy, D. Ron, and J.-R. Lee, "Energy efficiency optimization for SWIPT-based D2D-underlaid cellular networks using multiagent deep reinforcement learning," *IEEE Systems Journal*, pp. 1–9, 2021.

[13] H. Chen, L. Liu, H. S. Dhillon, and Y. Yi, "Qos-aware D2D cellular networks with spatial spectrum sensing: A stochastic geometry view," *IEEE Transactions on Communications*, vol. 67, no. 5, pp. 3651–3664, 2019.

[14] M. Farooq-I-Azam, W. Yu, Q. Ni, M. Dong, and A. ul Quddus, "Location assisted subcarrier and power allocation in underlay mobile cognitive radio networks," in *2018 IEEE Globecom Workshops (GC Wkshps)*, 2018, pp. 1–6.

[15] C.-L. Chuang, W.-Y. Chiu, and Y.-C. Chuang, "Dynamic multiobjective approach for power and spectrum allocation in cognitive radio networks," *IEEE Systems Journal*, pp. 1–12, 2021.

[16] X. Song, X. Meng, X. Shen, and C. Jia, "Cognitive radio networks with primary receiver assisted interference avoidance protocol," *IEEE Access*, vol. 6, pp. 1224–1235, 2018.

[17] C. Jia, X. Song, and X. Meng, "Fog-aided cognitive radio networks with guard zone and interference cancellation based opportunistic spectrum access," *IEEE Access*, vol. 6, pp. 59 182–59 191, 2018.

[18] L. Xiao, Y. Li, J. Liu, and Y. Zhao, "Power control with reinforcement learning in cooperative cognitive radio networks against jamming," *The Journal of Supercomputing*, vol. 71, no. 9, pp. 3237–3257, Sep 2015.

[19] Y. Cao, N. Zhao, F. R. Yu, M. Jin, Y. Chen, J. Tang, and V. C. M. Leung, "Optimization or alignment: Secure primary transmission assisted by secondary networks," *IEEE Journal on Selected Areas in Communications*, vol. 36, no. 4, pp. 905–917, 2018.

[20] B. Chen, Y. Chen, Y. Chen, Y. Cao, Z. Ding, N. Zhao, and X. Wang, "Secure primary transmission assisted by a secondary full-duplex NOMA relay," *IEEE Transactions on Vehicular Technology*, vol. 68, no. 7, pp. 7214–7219, 2019.

[21] T. Çavdar, E. Güler, and Z. Sadreddini, "Instant overbooking framework for cognitive radio networks," *Comput. Netw.*, vol. 76, no. C, p. 227–241, jan 2015.

[22] M. Farooq-I-Azam, Q. Ni, M. Dong, and H. B. Pervaiz, "Cooperative localization based interference avoidance in cognitive radio networks," in *ICC 2021 - IEEE International Conference on Communications*, 2021, pp. 1–6.

[23] T. Vongsuteera and K. Rojviboonchai, "Adaptive indoor localization system for large-scale area," *IEEE Access*, vol. 9, pp. 8847–8865, 2021.

[24] M. Farooq-I-Azam, Q. Ni, and E. A. Ansari, "Intelligent energy efficient localization using variable range beacons in industrial wireless sensor networks," *IEEE Transactions on Industrial Informatics*, vol. 12, no. 6, pp. 2206–2216, Dec 2016.

[25] W. Su, J. D. Matyjas, and S. Batalama, "Active cooperation between primary users and cognitive radio users in heterogeneous ad-hoc networks," *IEEE Transactions on Signal Processing*, vol. 60, no. 4, pp. 1796–1805, 2012.

[26] M. Liu, T. Song, J. Hu, H. Sari, and G. Gui, "Anti-shadowing resource allocation for general mobile cognitive radio networks," *IEEE Access*, vol. 6, pp. 5618–5632, 2018.

[27] W. Tranter, K. Kosbar, T. Rappaport, and K. Shanmugan, *Principles of Communication Systems Simulation with Wireless Applications*, ser. Prentice Hall communications engineering and emerging technologies series. Prentice Hall, 2004.

[28] X.-L. Huang, Y.-X. Li, Y. Gao, and X.-W. Tang, "Q-learning-based spectrum access for multimedia transmission over cognitive radio networks," *IEEE Transactions on Cognitive Communications and Networking*, vol. 7, no. 1, pp. 110–119, 2021.